NANO LETTERS

Letter

pubs.acs.org/NanoLett

Graphene Quantum Dots Derived from Carbon Fibers

Juan Peng,[†,‡] Wei Gao,[§] Bipin Kumar Gupta,[†,∥] Zheng Liu,[†] Rebeca Romero-Aburto,[†,⊥] Liehui Ge,[†] Li Song,[#] Lawrence B. Alemany,[§] Xiaobo Zhan,[†] Guanhui Gao,[†,▽] Sajna Antony Vithayathil,[○] Benny Abraham Kaipparettu,[○] Angel A. Marti,[§,♦] Takuya Hayashi,[+] Jun-Jie Zhu,*[,‡] and Pulickel M. Ajayan*[,†,§]

[†]Mechanical Engineering and Materials Science Department, Rice University, Houston, Texas 77005, United States

[‡]State Key Lab of Analytical Chemistry for Life Science, School of Chemistry and Chemical Engineering, Nanjing University, Nanjing 210093, P. R. China

[§]Department of Chemistry, Rice University, Houston, Texas 77005, United States

[∥]National Physical Laboratory (CSIR), Dr K S Krishnan Road, New Delhi 110012, India

[⊥]Department of Molecular Pathology, The University of Texas, MD. Anderson Cancer Center, Houston Texas 77054, United States

[#]Research Center for Exotic Nanocarbons, Shinshu University, 4-17-1 Wakasato, Nagano 380-8553, Japan

[▽]Institute of Materials Science and Engineering, Ocean University of China, Qingdao, 266003, P.R. China

[○]Department of Molecular and Human Genetics, Baylor College of Medicine, Houston, Texas 77030, United States

[♦]Department of Chemistry and Bioengineering, Rice University, Houston, Texas 77005, United States

[+]Faculty of Engineering, Shinshu University, 4-17-1 Wakasato, Nagano 380-8553, Japan

Supporting Information

ABSTRACT: Graphene quantum dots (GQDs), which are edge-bound nanometer-size graphene pieces, have fascinating optical and electronic properties. These have been synthesized either by nanolithography or from starting materials such as graphene oxide (GO) by the chemical breakdown of their extended planar structure, both of which are multistep tedious processes. Here, we report that during the acid treatment and chemical exfoliation of traditional pitch-based carbon fibers, that are both cheap and commercially available, the stacked graphitic submicrometer domains of the fibers are easily broken down, leading to the creation of GQDs with different size distribution in scalable amounts. The as-produced GQDs, in the size range of 1−4 nm, show two-dimensional morphology, most of which present zigzag edge structure, and are 1−3 atomic layers thick. The photoluminescence of the GQDs can be tailored through varying the size of the GQDs by changing process parameters. Due to the luminescence stability, nanosecond lifetime, biocompatibility, low toxicity, and high water solubility, these GQDs are demonstrated to be excellent probes for high contrast bioimaging and biosensing applications.

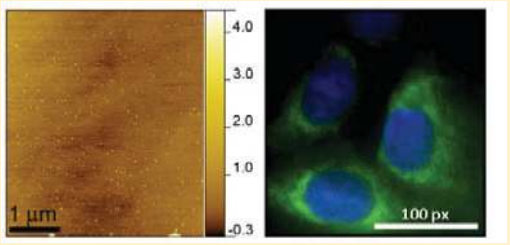

KEYWORDS: *Graphene quantum dots, carbon fibers, zigzag edge, luminescence, imaging*

Graphene has attracted much attention because of its unique physical properties and with numerous promising applications in nanotechnology.[1−9] However, graphene is a zero-bandgap semiconductor, which limits its electronic and opto-electronic application.[10] Due to the lack of a bandgap, no optical luminescence is observed in pristine graphene. A bandgap, however, can be engineered into graphene nanoribbons (GNRs) and graphene quantum dots (GQDs) due to quantum confinement[11,12] and edge effects.[13] Most works on GQDs have been focused on theoretical prediction;[12,14−17] however, the experimental synthesis and characterization of GQDs is only a recent effort. Apart from graphene materials, the photoluminescence (PL) in carbon based nanostructures such as fullerene,[18] carbon nanotubes,[19−21] nanodiamond,[22,23] and carbon nanoparticles[24−26] has been studied extensively with potential applications such as fluorescent probes for bioimaging due to their biocompatibility under the physiological condition.[27−29]

GQDs have been fabricated by electro-beam lithography[11] or ruthenium-catalyzed C_{60} transformation.[30] These methods are limited by the requirement for special equipment, extremely expensive raw materials and low yield. Recently, GQDs have been prepared through hydrothermal[31] or electrochemical strategies,[32] showing blue or green luminescence. However, these methods are based on starting materials such as graphene oxide (GO) and its reduction product, which is typically synthesized from oxidation of bulk graphite powders via a series

Received: November 5, 2011
Revised: December 17, 2011
Published: January 4, 2012

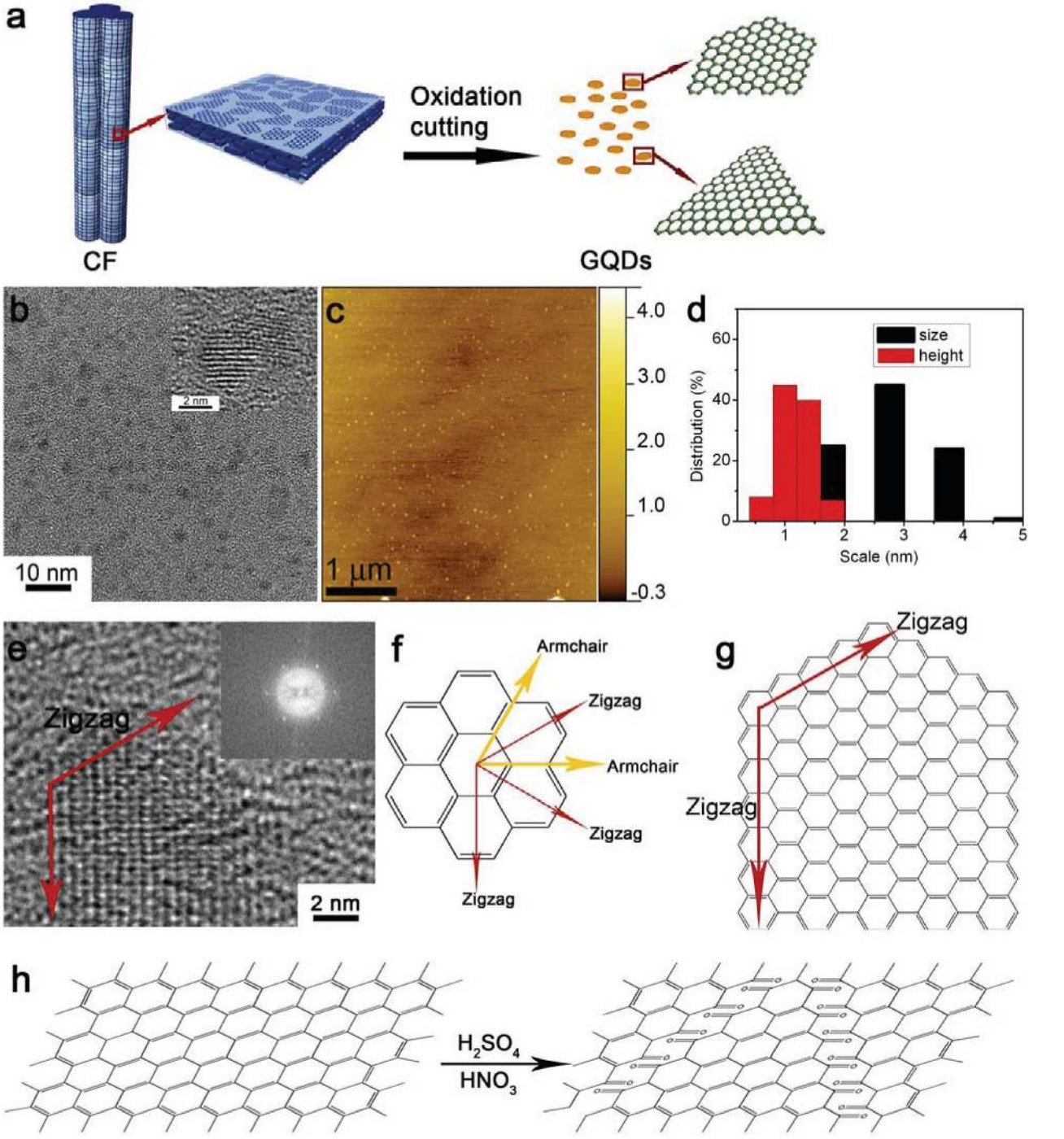

Figure 1. (a) Representation scheme of oxidation cutting of CF into GQDs. (b) TEM images of GQDs (synthesized reaction temperature at 120 °C), inset of (b) is the HRTEM of GQDs. (c) AFM image of GQDs. (d) Size and height distribution of GQDs. (e) HRTEM image of the edge of GQD, inset is the 2D FFT of the edge in (e). (f) Schematic illustration showing the orientation of the hexagonal graphene network and the relative zigzag and armchair directions. (g) Schematic representation of the edge termination of the HRTEM image in (e). (h) Proposed mechanism for the chemical oxidation of CF into GQDs.

of chemical treatments which typically take several days and involve lots of chemical reagents. In addition, these methods offered the GQDs with only one emission color (blue or green luminescence). Since the bandgap depends on size,[33] shape,[34] and fraction of the sp^2 domains,[6] PL emission can be tuned by controlling the nature and size of the extended sp^2 sites.[35] It will be easier to get size controlled synthesis of GQDs if the starting material already has small domain structure of the sp^2 carbons and these can be easily extracted. It is reported that graphene oxide nanocolloids can be made from graphite nanofibers.[36] Here we report a facile one-step wet chemically derived GQDs from acidic treatment of carbon fibers (CF), which have a resin-rich surface. Interestingly, the photoluminescence from these CF derived GQDs can be tailored by simply choosing different reaction temperatures which effectively produces GQDs of varying sizes.

The GQDs are synthesized by chemical oxidation and cutting of micrometer-sized pitch-based carbon fibers (CF), the

dx.doi.org/10.1021/nl2038979 | Nano Lett. 2012, 12, 844–849

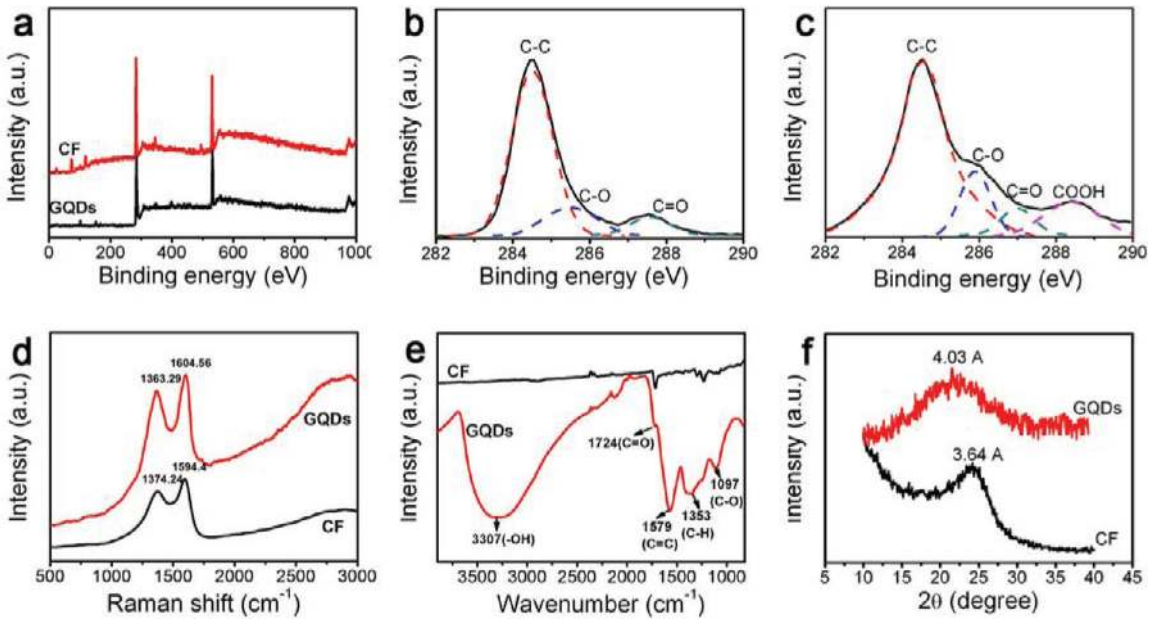

Figure 2. (a) XPS survey spectrum of CF and GQDs. (b) High-resolution XPS C1s spectra of CF. (c) The XPS C1s spectra of GQDs. (d) Raman spectra of CF and GQDs. (e) FTIR spectra of CF and GQDs. (f) XRD pattern of CF and GQDs.

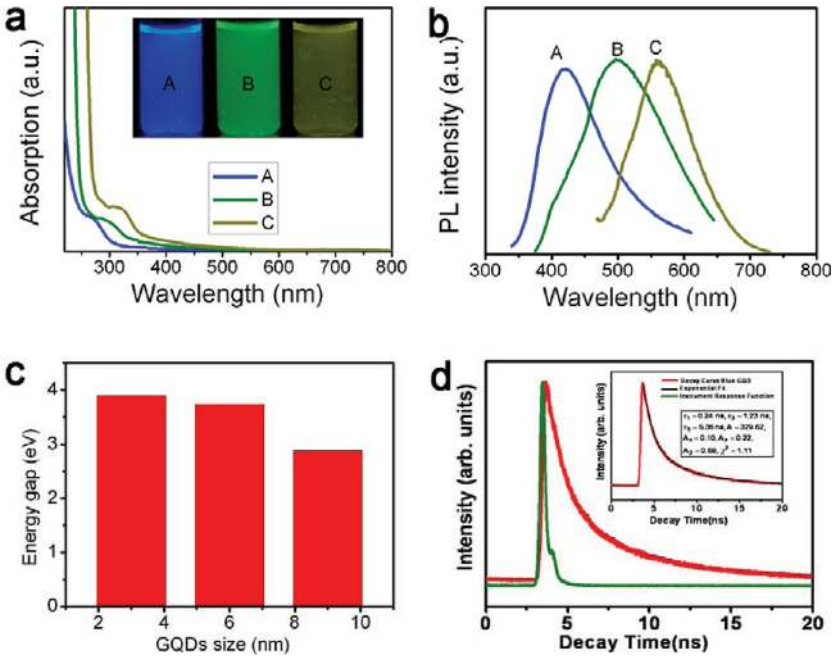

Figure 3. Optical properties of the GQDs. (a) UV−vis spectra of GQDs A, B, and C, corresponds to synthesized reaction temperature at 120, 100, and 80 °C, respectively. Inset of panel a is a photogaph of the corresponding GQDs under UV light with 365 nm excitation. (b) PL spectra of GQDs with different emission color excited at 318, 331, and 429 nm, respectively. (c) Relationship between the energy gap and the size of GQDs. (d) TRPL decay profile of blue GQDs recorded at room temperature. The inset shows the lifetime data and the parameter generated by the exponential fitting.

scheme is shown in Figure 1a (see Methods Summary for the details and Figure S1 in the Supporting Information for the SEM images of CF). The as-synthesized GQDs are highly soluble in water and other polar organic solvents, such as dimethylformamide (DMF) and dimethyl sulfoxide (DMSO). The pictures of the GQDs dispersed in DMF and DMSO are shown in Figure S2 in the Supporting Information. Figure 1b show a TEM image of the fiber derived GQDs (synthesized reaction temperature at 120 °C), showing relatively a narrow size distribution between 1 and 4 nm, which are summarized in Figure 1d. The high resolution TEM (HRTEM) image (inset of Figure 1b) indicates high crystallinity of the GQDs, with a lattice parameter of 0.242 nm, (1120) lattice fringes of graphene. The AFM image in Figure 1c demonstrates the topographic morphology of GQDs, the heights of which are between 0.4 and 2 nm, corresponding to 1−3 graphene layers. Characterization of the edge structure (e.g., zigzag and armchair edges[37]) in graphene is very important for the understanding of the GQD properties. It has been reported that graphene with zigzag edges offers specific electronic or magnetic proper-

dx.doi.org/10.1021/nl2038979 | Nano Lett. 2012, 12, 844−849

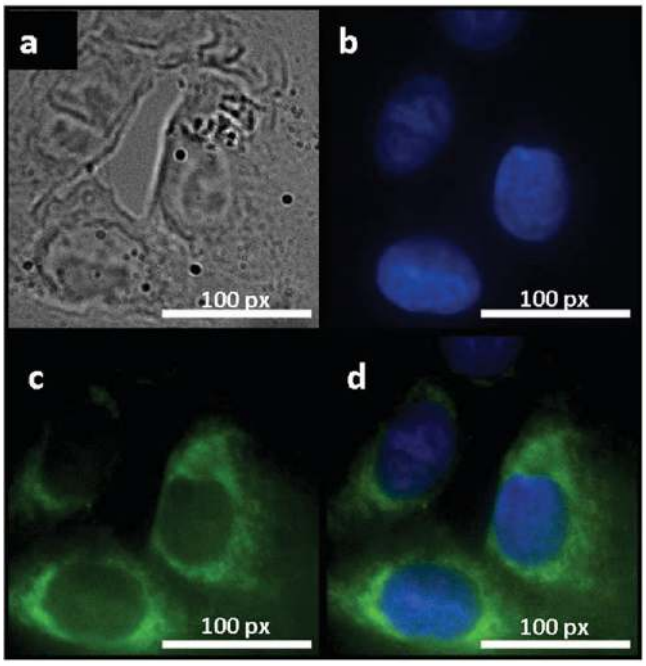

Figure 4. Fluorescent images of human breast cancer cell T47D after incubation with green GQDs for 4 h (a) phase contrast picture of T47D cells. (b) Individual nucleus stained blue with DAPI. (c) Agglomerated green GQDs surrounding each nucleus. (d) The overlay high contrast image of nucleolus stained with blue DAPI and GQDs (green) staining.

ties.[37−39] Figure 1e shows the HRTEM image of the edge structure of a GQD. The corresponding fast Fourier transform (FFT) pattern is shown in the inset of Figure 1e. From the 2D FFT image, a schematic model is shown in Figure 1f, to show the orientation of the hexagonal graphene network and the relative zigzag and armchair directions. The GQD edges seem to be predominantly parallel to the zigzag orientation (red arrows in Figure 1e), although other orientations are also possible. A schematic suggesting the structure of this GQD is shown in Figure 1g. From a large number of GQDs we have analyzed, it seems that the GQDs made here prefer zigzag edges more than armchair ones. The formation of the GQDs depends on how the submicrometer domain structure of the sp^2 carbons, present in the carbonized pitch fiber structure, is broken down. Carbon nanotubes have been unzipped to produce graphene nanoribbons by chemical oxidation routes and the unzipping mechanism has been proposed.[40] Similarly, here, the breakup of the fiber structure and the planar graphitic domains is chemically initiated by the lining up of chemical functionalities (such as epoxy or carbonyl groups)[41] making the graphitic domains prone to fracture, preferably along the zigzag direction (Figure 1h).

XPS measurements were carried out to probe the composition of GQDs. As seen in Figure 2a, the XPS show a dominant graphitic C_{1s} peak at 284.8 eV and O_{1s} peak at ca. 532 eV for original CF and GQDs. The C:O atomic ratios in CF and GQDs are 6.52 and 3.22, respectively. The comparison of the high-resolution spectra of C_{1s} (Figure 2, panels b and c) demonstrates the obvious change in carbon chemical environment from CF to GQDs. The presence of C═C, C−O, C═O, and COOH bonds in Figure 2c, indicated GQD_S were functionalized with hydroxyl, carbonyl, and carboxylic acid groups. Raman spectroscopy was also used to characterize the GQDs, as shown in Figure 2d. The G peak shows blue shift compared with the original CF. The 2D peak of GQDs can be found at 2700 cm^{-1}. The relative intensity of the "disorder" D band to the crystalline G-band (I_D/I_G) for the GQDs is 0.91, which is higher than that of GQDs prepared by electrochemical routes.[32] During the oxidation, oxygen-containing groups, including carbonyl, carboxyl, hydroxyl, and epoxy groups were introduced to the edges and onto the basal plane, as shown in the Fourier transform infrared (FTIR) spectrum (Figure 2e). The presence of these groups makes the GQDs soluble in water. Figure 2f shows the typical XRD profiles for CF and GQDs. The GQDs have a broader (002) peak centered at around 21.5 degrees. The interlayer spacing is 0.403 nm, which is broader than that of graphite.[42] The XRD peak for GQDs shifted to a lower degree compared with the CF, indicating that GQDs had a bigger interlayer spacing than that of the original CF (0.364 nm). This result could be attributed to the oxygen-containing groups introduced in the exfoliation and oxidation of CF, which enhanced the interlayer distance. However, the interlayer distance of GQDs is smaller than the graphene oxide,[43] which could be explained that GQDs are only oxidized on the edges due to the very small size.

Figure 3a shows the UV−visible absorption spectra of GQDs synthesized at temperatures of 80, 100, and 120 °C, respectively. A clear blue shift from 330 to 270 nm with increasing the temperature is observed. The result reveals that the reaction temperature can affect the absorption properties of as-sythesized GQDs and that lower temperature leads to GQDs absorption at longer wavelenths. The inset of Figure 3a shows the optical images of three GQDs under UV light. The GQDs with synthesized temperatures of 120, 100, and 80 °C show blue, green, and yellow emission colors, respectively. The color coordinates of GQDs are shown in Figure S3 (see the Supporting Information). Figure 3b shows the corresponding emission spectra of as-prepared GQDs to Figure 3a. The result reveals that the temperature can change the distribution of emission wavelength of as-synthesized GQDs. Different emission color may originate from GQDs of different size, shape and defects.[16] Further characterization (typical TEM images and size distribution for green and yellow GQDs, see Figure S4 in the Supporting Information) supports the conclusion that different-sized GQDs yield different emission colors. The optical properties of GQDs vary with the GQDs size which could also result in the variation in density and nature of sp^2 sites available in GQDs. Thus the energy gap of GQDs can be tuned by changing the size of GQDs. Figure 3c shows the relationship between the energy gap and the GQDs size. It is clearly seen that the energy gap decreases from 3.90 to 2.89 eV with increasing the size, which corresponds to the same kind of trend observed in other quantum dots due to the quantum confinement effect at lower particle sizes (1−10 nm).[44] The photoluminescence excitation (PLE) spectra of the blue GQDs (λ_{em} = 434 nm) as well as PL spectra is shown in Figure S5 (see the Supporting Information). The PLE spectra shows two sharp peaks at 284 and 318 nm. The PLE spectra clearly demonstrates that the observed luminescence from the GQDs could be correlate with the two new transitions at 284 and 318 nm rather than the commonly observed $\pi-\pi^*$ transition. The two electronic transitions of 318 nm (3.89 eV) and 284 nm (4.36 eV) observed in the PLE spectra (Figure S5) can be considered as a transition from the σ and π orbital (HOMO) to the lowest unoccupied molecular orbital (LUMO), as demonstrated in Figure S6. The PLE spectra of

dx.doi.org/10.1021/nl2038979 | Nano Lett. 2012, 12, 844−849

green and yellow GQDs are shown in Figures S7 and S8, respectively, which also show two sharp peaks. The carbine ground-state multiplicity is related to energy differences (δE) between the σ and π orbital. δE should be below 1.5 eV for a triplet ground state.[45,46] In our work here, the δEs for GQDs with blue, green and yellow emission are 0.47, 0.82, and 1.24 eV, respectively. The data show that the δEs within the required value for triple carbenes. The luminescence is the irradiation decay of activated electrons from the LUMO to the HOMO. All of the obtained GQDs exhibit excitation dependent PL behaviors. Here, we explored such behavior of blue GQDs. When blue GQDs are excited at wavelengths from 318 to 420 nm, the PL peak shifts from 434 to 503 nm and the PL intensity decreased remarkably (Figure S9). To further analyze the chemical environment dependence PL behavior of blue GQDs, we performed the pH dependent PL to vary the pH value from 1 to 13. Figure S10 exhibits the PL spectra of blue GQDs at different pH. The pH dependent PL emission results reveal that, under alkaline conditions, the blue GQDs emit strong PL, whereas under acidic conditions, the PL intensity decreases. This result would be attributed to the following explanations. The free zigzag sites of the GQDs are protonated and a complex between the zigzag sites and H^+ is formed in acidic solution. Thus, the emissive state becomes inactive in PL.

The luminescence decay profiles of the blue GQDs are shown in Figure 3d. The decay were recorded for the GQDs transitions at 434 nm for blue and 500 nm for green emission at 371 nm excitation measured at room temperature by a time-correlated single photon counting technique. The lifetime data of blue and green GQDs were very well fitted to a triple-exponential function as shown in Figure 3d and Figure S11 (see the Supporting Information). The parameters generated from iterative reconvolution of the decay with the instrument response function (IRF) are listed in the inset of Figures 3d and S10 for blue and green GQDs, respectively. The observed lifetimes of the blue quantum dot are τ_1 = 0.24 ns, τ_2 = 1.23 ns, and τ_3 = 5.36 ns, whereas for green GQDs lifetime τ_1 = 0.26 ns, τ_2 = 1.15 ns, and τ_3 = 4.30 ns were observed. The observed lifetime of GQDs in nanosecond suggests that the synthesized GQDs are most suitable for optoelectronic and biological applications.

As hypothesized, GQDs could be used for biological applications such as bioimaging, protein analysis by FRET, cell tracking, isolation of biomolecules, and gene technology, among others if the inherent toxicity of the material allows it. Therefore the cytotoxicity of GQDs (green or blue) was evaluated using two different human breast cancer cell lines MDA-MB-231 and T47D with MTT viability assay. As observed in Figure S12 (see the Supporting Information), low doses of GQDs (up to 50 μg/mL) do not impose a considerable toxicity to these cells compared to the control (untreated). 1 μM of doxorubicin was used as a positive control, toxicity at 24 and 48 h is 50% and 35%, respectively (see Figure S13 in the Supporting Information). Cell proliferation at low dosage as the exposure time increases is not affected in accordance to Figure S12. The experimental method of MTT assay is described in the Supporting Information.

To determine whether GQDs can be used for cellular imaging, we chose the green GQDs because the nucleus was stained with mounting medium with DAPI (blue color) cell's nucleus showing blue color under imaging. We have performed in vitro cellular studies using human breast cancer cell lines T47D. The cells were cultured and maintained in DMEM medium as described in the Supporting Information. Figure 4 shows the images of T47D cells treated with green GQDs for 4 h incubation time. The obtained images clearly visualize the phase contrast image of T47D cells, nucleus stained blue with DAPI, agglomerated high contrast fluorescent image of green GQDs around each nucleus and overlay image of cell with phase contrast, DAPI and green GQDs. These obtained images indicate that GQDs can be used in high contrast bioimaging and other biomedical applications.

In conclusion, we have demonstrated a facile synthesis of GQDs in large scale with acidic exfoliation and etching of pitch carbon fibers, which are rich in distributed graphitic domains in their original frameworks. The size of the as-prepared GQDs varies with the reaction temperature, and the emission color and the bandgap of GQDs can be controlled accordingly. We have also shown the low cytotoxicity and excellent biocompatibility of these GQDs, thus they can be used as an eco-friendly material in biolabeling and bioimaging. Furthermore, our GQDs with tunable photoluminescence could also find promising applications in opto-electronics.

■ ASSOCIATED CONTENT

Ⓢ Supporting Information

Experimental details for GQDs synthesis method, characterization tools, cytotoxicity evaluation, and cell imaging. SEM images of CF. Additional GQDs characterization data including TEM images, PLE, PL spectra, TRPL decay profile and the cell viability assay results. This material is available free of charge via the Internet at http://pubs.acs.org.

■ AUTHOR INFORMATION

Corresponding Author

*E-mail: ajayan@rice.edu (P.M.A.); jjzhu@nju.edu.cn (J.-J.Z.).

■ ACKNOWLEDGMENTS

J.P. and J.J.Z. appreciate the support of NSFC (21020102038 and 21121091) and National Basic Research Program of China (2011CB933502). W.G. and P.M.A. acknowledge funding support from Nanoholdings. P.M.A. and Z.L. acknowledge funding support from the Office of Naval Research (ONR) through the MUR1 program on graphene. B.K.G. thanks financial support from Indo-US Science and Technology Forum (IUSSTF), Award No. Indo-US Research Fellowship/2010-2011/25-2010. A.A.M. thanks the Welch foundation (C-1743) for financial support.

■ REFERENCES

(1) Geim, A. K.; Novoselov, K. S. The rise of graphene. *Nat. Mater.* **2007**, *6*, 183−191.

(2) Choucair, M.; Thordarson, P.; Stride, J. A. Gram-scale production of graphene based on solvothermal synthesis and sonication. *Nat. Nanotechnol.* **2009**, *4*, 30−33.

(3) Li, D.; Muller, M. B.; Gilje, S.; Kaner, R. B.; Wallace, G. G. Processable aqueous dispersions of graphene nanosheets. *Nat. Nanotechnol.* **2008**, *3*, 101−105.

(4) Li, X. L.; Wang, X. R.; Zhang, L.; Lee, S. W.; Dai, H. J. Chemically derived, ultrasmooth graphene nanoribbon semiconductors. *Science* **2008**, *319*, 1229−1232.

(5) Zhu, Y.; et al. Graphene and Graphene Oxide: Synthesis, Properties, and Applications. *Adv. Mater.* **2010**, *22*, 3906−3924.

(6) Eda, G.; et al. Blue Photoluminescence from Chemically Derived Graphene Oxide. *Adv. Mater.* **2010**, *22*, 505−508.

(7) Green, A. A.; Hersam, M. C. Solution Phase Production of Graphene with Controlled Thickness via Density Differentiation. *Nano Lett.* **2009**, *9*, 4031−4036.
(8) Terrones, M.; et al. Graphene and graphite nanoribbons: Morphology, properties, synthesis, defects and applications. *Nano Today* **2010**, *5*, 351−372.
(9) Loh, K. P.; Bao, Q.; Eda, G.; Chhowalla, M. Graphene oxide as a chemically tunable platform for optical applications. *Nat. Chem.* **2010**, *2*, 1015−1024.
(10) Novoselov, K. S.; et al. Electric field effect in atomically thin carbon films. *Science* **2004**, *306*, 666−669.
(11) Ponomarenko, L. A.; et al. Chaotic dirac billiard in graphene quantum dots. *Science* **2008**, *320*, 356−358.
(12) Li, L. S.; Yan, X. Colloidal Graphene Quantum Dots. *J. Phys. Chem. Lett.* **2010**, *1*, 2572−2576.
(13) Zhu, S. J.; et al. Strongly green-photoluminescent graphene quantum dots for bioimaging applications. *Chem. Commun.* **2011**, *47*, 6858−6860.
(14) Mueller, M. L.; Yan, X.; Dragnea, B.; Li, L. S. Slow Hot-Carrier Relaxation in Colloidal Graphene Quantum Dots. *Nano Lett.* **2011**, *11*, 56−60.
(15) Mueller, M. L.; Yan, X.; McGuire, J. A.; Li, L. S. Triplet States and Electronic Relaxation in Photoexcited Graphene Quantum Dots. *Nano Lett.* **2010**, *10*, 2679−2682.
(16) Yan, X.; et al. Independent Tuning of the Band Gap and Redox Potential of Graphene Quantum Dots. *J. Phys. Chem. Lett* **2011**, *2*, 1119−1124.
(17) Gueclue, A. D.; Potasz, P.; Hawrylak, P. Excitonic absorption in gate-controlled graphene quantum dots. *Phys. Rev. B*, **2010**, *82*.
(18) Jeong, J.; Cho, M.; Lim, Y. T.; Song, N. W.; Chung, B. H. Synthesis and Characterization of a Photoluminescent Nanoparticle Based on Fullerene-Silica Hybridization. *Angew. Chem. Int. Ed.* **2009**, *48*, 5296−5299.
(19) Welsher, K.; et al. A route to brightly fluorescent carbon nanotubes for near-infrared imaging in mice. *Nat. Nanotechnol.* **2009**, *4*, 773−780.
(20) Ju, S. Y.; Kopcha, W. P.; Papadimitrakopoulos, F. Brightly Fluorescent Single-Walled Carbon Nanotubes via an Oxygen-Excluding Surfactant Organization. *Science* **2009**, *323*, 1319−1323.
(21) Riggs, J. E.; Guo, Z. X.; Carroll, D. L.; Sun, Y. P. Strong luminescence of solubilized carbon nanotubes. *J. Am. Chem. Soc.* **2000**, *122*, 5879−5880.
(22) Mochalin, V. N.; Gogotsi, Y. Wet Chemistry Route to Hydrophobic Blue Fluorescent Nanodiamond. *J. Am. Chem. Soc.* **2009**, *131*, 4594−4595.
(23) Nish, A.; Hwang, J. Y.; Doig, J.; Nicholas, R. J. Highly selective dispersion of singlewalled carbon nanotubes using aromatic polymers. *Nat. Nanotechnol.* **2007**, *2*, 640−646.
(24) Zheng, L. Y.; Chi, Y. W.; Dong, Y. Q.; Lin, J. P.; Wang, B. B. Electrochemiluminescence of Water-Soluble Carbon Nanocrystals Released Electrochemically from Graphite. *J. Am. Chem. Soc.* **2009**, *131*, 4564−4565.
(25) Sun, Y. P.; et al. Quantum-sized carbon dots for bright and colorful photoluminescence. *J. Am. Chem. Soc.* **2006**, *128*, 7756−7757.
(26) Zhou, J. G.; et al. An electrochemical avenue to blue luminescent nanocrystals from multiwalled carbon nanotubes (MWCNTs). *J. Am. Chem. Soc.* **2007**, *129*, 744−745.
(27) Cao, L.; et al. Carbon dots for multiphoton bioimaging. *J. Am. Chem. Soc.* **2007**, *129*, 11318−11319.
(28) Chandra, S.; Das, P.; Bag, S.; Laha, D.; Pramanik, P. Synthesis, functionalization and bioimaging applications of highly fluorescent carbon nanoparticles. *Nanoscale* **2011**, *3*, 1533−1540.
(29) Ray, S. C.; Saha, A.; Jana, N. R.; Sarkar, R. Fluorescent Carbon Nanoparticles: Synthesis, Characterization, and Bioimaging Application. *J. Phys. Chem. C* **2009**, *113*, 18546−18551.
(30) Lu, J.; Yeo, P. S. E.; Gan, C. K.; Wu, P.; Loh, K. P. Transforming C_{60} molecules into graphene quantum dots. *Nat. Nanotechnol.* **2011**, *6*, 247−252.
(31) Pan, D. Y.; Zhang, J. C.; Li, Z.; Wu, M. H. Hydrothermal Route for Cutting Graphene Sheets into Blue-Luminescent Graphene Quantum Dots. *Adv. Mater.* **2010**, *22*, 734−738.
(32) Li, Y.; et al. An Electrochemical Avenue to Green-Luminescent Graphene Quantum Dots as Potential Electron-Acceptors for Photovoltaics. *Adv. Mater.* **2011**, *23*, 776−779.
(33) Li, H.; et al. Water-Soluble Fluorescent Carbon Quantum Dots and Photocatalyst Design. *Angew. Chem., Int. Ed.* **2010**, *49*, 4430−4434.
(34) Yan, X.; et al. Independent Tuning of the Band Gap and Redox Potential of Graphene Quantum Dots. *J. Phys. Chem. Lett.* **2011**, *2*, 1119−1124.
(35) Yan, X.; Cui, X.; Li, L. S. Synthesis of Large, Stable Colloidal Graphene Quantum Dots with Tunable Size. *J. Am. Chem. Soc.* **2010**, *132*, 5944−5945.
(36) Luo, J. Y.; Cote, L. J.; Tung, V. C.; Tan, A. T. L.; Goins, P. E.; Wu, J. S.; Huang, J. X. Graphene oxide nanocolloids. *J. Am. Chem. Soc.* **2010**, *132*, 17667−17669.
(37) Radovic, L. R.; Bockrath, B. On the chemical nature of graphene edges: Origin of stability and potential for magnetism in carbon materials. *J. Am. Chem. Soc.* **2005**, *127*, 5917−5927.
(38) Gusynin, V. P.; Miransky, V. A.; Sharapov, S. G.; Shovkovy, I. A.; Wyenberg, C. M. Edge states on graphene ribbons in magnetic field: Interplay between Dirac and ferromagnetic-like gaps. *Phys. Rev. B* **2009**, *79*.
(39) Nakada, K.; Fujita, M.; Dresselhaus, G.; Dresselhaus, M. S. Edge state in graphene ribbons: Nanometer size effect and edge shape dependence. *Phys. Rev. B* **1996**, *54*, 17954−17961.
(40) Kosynkin, D. V.; et al. Longitudinal unzipping of carbon nanotubes to form graphene nanoribbons. *Nature* **2009**, *458*, 872−875.
(41) Li, Z.; Zhang, W.; Luo, Y.; Yang, J.; Hou, J. G. How Graphene Is Cut upon Oxidation? *J. Am. Chem. Soc.* **2009**, *131*, 6320−6321.
(42) Guo, H.-L.; Wang, X.-F.; Qian, Q.-Y.; Wang, F.-B.; Xia, X.-H. A Green Approach to the Synthesis of Graphene Nanosheets. *ACS Nano* **2009**, *3*, 2653−2659.
(43) Moon, I. K.; Lee, J.; Ruoff, R. S.; Lee, H. Reduced graphene oxide by chemical graphitization. *Nat. Commun.* **2010**, *1*.
(44) Melnikov, D. V.; Chelikowsky, J. R. Quantum confinement in phosphorus-doped silicon nanocrystals. *Phys. Rev. Lett.* **2004**, *92*.
(45) Bourissou, D.; Guerret, O.; Gabbai, F. P.; Bertrand, G. Stable carbenes. *Chem. Rev.* **2000**, *100*, 39−91.
(46) Hoffmann, R. Trimethylene and addition of methyelene to ethylene. *J. Am. Chem. Soc.* **1968**, *90*, 1475−1476.